Cell, Vol. 103, 645–654, November 10, 2000, Copyright ©2000 by Cell Press

Structure of Bax: Coregulation of Dimer Formation and Intracellular Localization

Motoshi Suzuki,* Richard J. Youle,* and Nico Tjandra†‡

*Biochemistry Section
Surgical Neurology Branch
National Institute of Neurological Disorders and Stroke
†Laboratory of Biophysical Chemistry
National Heart, Lung, and Blood Institute
National Institutes of Health
Bethesda, Maryland 20892

Summary

Apoptosis is stimulated by the insertion of Bax from the cytosol into mitochondrial membranes. The solution structure of Bax, including the putative transmembrane domain at the C terminus, was determined in order to understand the regulation of its subcellular location. Bax consists of 9 α helices where the assembly of helices α1 through α8 resembles that of the apoptosis inhibitor, Bcl-x_L. The C-terminal α9 helix occupies the hydrophobic pocket proposed previously to mediate heterodimer formation and bioactivity of opposing members of the Bcl-2 family. The Bax structure shows that the orientation of helix α9 provides simultaneous control over its mitochondrial targeting and dimer formation.

Introduction

Organ development and tissue turnover depend on the finely tuned regulation of programmed cell death or apoptosis. The Bcl-2 family of proteins that controls apoptosis is divided into three subfamilies (Adams and Cory, 1998; Gross et al., 1999). The subfamily including Bcl-2 and Bcl-x_L inhibits apoptosis whereas the Bax subfamily consisting of Bax and Bak as well as the BH3-only subfamily including Bid and Bad promote apoptosis. Functional studies have identified the importance of conserved Bcl-2 homology domains (BH1, BH2, BH3, and BH4) in many family members and a hydrophobic region in the C terminus predicted to be a membrane-spanning domain. Members of the Bcl-2 family form homo- and heterodimers under certain conditions. Based on the opposing functions of the members of this family, a model has been proposed in which dimerization of the pro- and antiapoptotic members controls their activity (Oltvai et al., 1993). The BH3 domain of proapoptotic members appears to be required for both the killing activity and dimer formation, although dimerization does not always correlate with the killing activity (Wang et al., 1998). The structure of a complex between Bcl-x_L and a Bak BH3 peptide provides some information on the possible interaction between different members of the Bcl-2 family (Sattler et al., 1997), and mutations at the binding site provide some clues on how dimerization might affect Bcl-x_L function (Minn et al., 1999). Despite strong evidence of specific molecular interaction between proteins in the Bcl-2 family, it is still unclear how this general scheme of control through interaction between pro- and antiapoptosis members is regulated.

The subcellular location of some Bcl-2 family members also appears to regulate their function. Bcl-2 and a fraction of Bcl-x_L can be found on the mitochondrial outer membrane. In contrast, Bax exists predominantly in the cytosol before apoptosis induction (Hsu et al., 1997; Wolter et al., 1997). Early during apoptosis, Bax translocates from the cytosol to mitochondria (Hsu et al., 1997; Wolter et al., 1997) where it participates in mitochondrial disruption and the release of cytochrome c (Green and Reed, 1998). Modulating the insertion step can regulate apoptosis (Goping et al., 1998; Gross et al., 1998; Nechushtan et al., 1999). To understand the molecular mechanism by which human Bax regulates apoptosis, we have determined its solution structure by nuclear magnetic resonance spectroscopy (NMR).

Results

Bax Structure

The structure was determined from the combination of experimental nuclear Overhauser effects (NOEs) and dipolar coupling restraints using methods largely developed by Bax and coworkers (Tjandra and Bax, 1997; Clore et al., 1998; Cornilescu et al., 1998; Ottiger et al., 1998). The structure of Bax consists of nine α helices (Figure 1). The overall fold of Bax closely resembles that of Bcl-x_L (Muchmore et al., 1996) with eight amphipathic α helices clustered around one central hydrophobic α helix (α5). The backbone relaxation data provide good indication that Bax exists as a monomer in solution as the average ^{15}N T_2 values for residues in regular secondary structures is characteristic for a protein of this size (Figure 2). The backbone $^{15}N\{^1H\}$-NOE and ^{15}N T_2 can be used to identify flexible regions in the protein. The characteristically low $^{15}N\{^1H\}$-NOE and a marked increase in the ^{15}N T_2 indicate that the N-terminal 12 residues are highly mobile. The C^α and C^β chemical shifts for these residues are close to their random coil values. This region, therefore, does not adopt an ordered conformation in solution. The large loop located between helix α1 and α2, also seen in Bcl-x_L (Muchmore et al., 1996) and Bid (Chou et al., 1999; McDonnell et al., 1999), is quite flexible except for the center region (Glu^{44}-Ala^{46}). The backbone relaxation rates for these central residues are close to the average values for residues in the rigid part of the molecule (Figure 2). In addition, weak NOEs were observed between these central residues and Ile^{133} as well as Met^{137} of helix α6. These indicate that, for a significant fraction of time, the center part of this loop contacts the globular part of the protein. The dynamic profile of this long loop is similar to the corresponding one in Bcl-x_L (residues Lys^{21}–Met^{83}). In Bcl-x_L, the region between residue Ala^{50} and Ala^{60} exhibited $^{15}N\{^1H\}$-NOE

‡To whom correspondence should be addressed (e-mail: nico@helix.nih.gov).

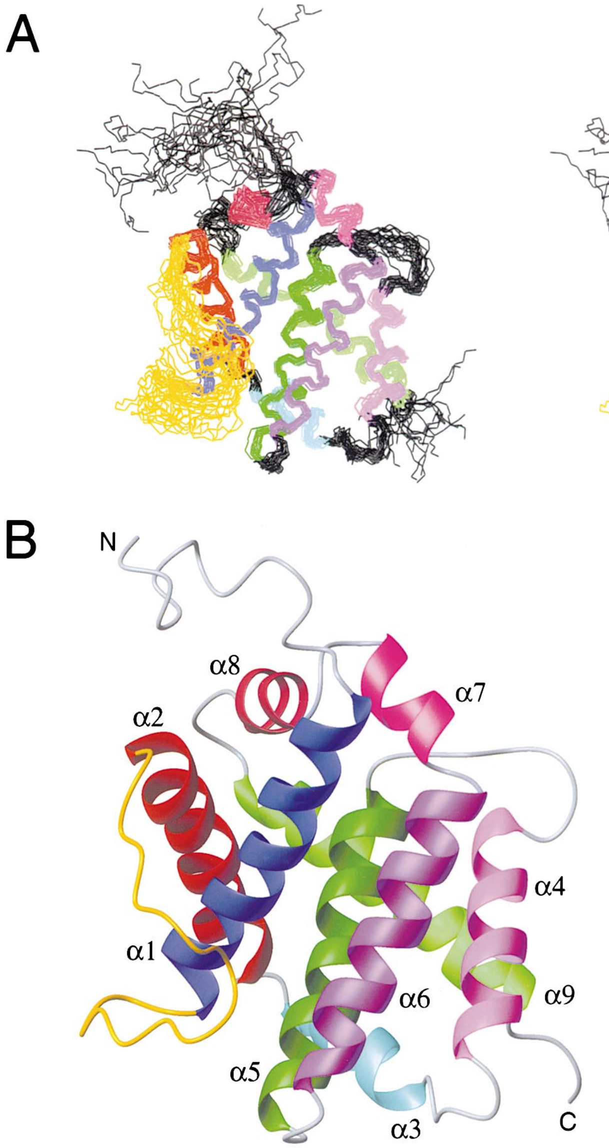

D

```
              *     *    ***    *
Bcl-2     93  VHLTLRQAGDDFSRR  107
Bcl-xL    86  VKQALREAGDEFELR  100
MCL      209  TAARLKALGDELHQR  223
Bax       59  LSECLKRIGDELDSN   73
Bak       74  VGRQLAIIGDDINRR   88
Bid       86  IARHLAQVGDSMDRS  100
Bik       57  LALRLACIGDEMDVS   71
HRK       33  TAARLKALGDELHQR   47
Bad      110  YGRELRRMSDEFVDS  124
```

C

```
                                      α1
Bax      1  MDGSGEQPRGGGPTSSEQIMKTGALLLQGFIQDRA-----------------GRMGGEAPELALD  48
Bcl-xL   1                    MSQSNRELVVDFLSYKLSQKGYSWSQFSDVEENRTEAPEGTESEMET  47
                                 BH4

                                                             α2              α3
Bax     49  -----------------------------PVPQDASTKKLSECLKRIGDELDSN---MELQRMIAA  82
Bcl-xL  48  PSAINGNPSWHLADSPAVNGATGHSSSLDAREVIPMAAVKQALREAGDEFELRYRRAFSDLTSQL  113
                                                  BH3

                       α4                α5                  α6
Bax     83  VDT-DSPREVFFRVAADMFSDGNFNWGRVVALFYFASKLVLKALCTKVPELIRTIMGWTLDFLRE  146
Bcl-xL 114  HITPGTAYQSFEQVVNELFRDG-VNWGRIVAFFSFGGALCVESVDKEMQVLVSRIAAWMATYLND  176
                             BH1

              α7     α8                     α9
Bax    147  RLLGWIQDQGGWDGLLSYFGTPT-------------WQTVTIFVAGVLTASLTIWKKMG  192
Bcl-xL 177  HLEPWIQENGGWDTFVELYGNNAAAESRKGQERFNRWFLTGMTVAGVVLLGSLFSRK  233
                   BH2
```

Figure 1. Structure of Bax

(A) A stereo view of the backbone (N, C^{α}, C′, and O) superposition of 20 NMR derived structures of Bax. The long loop (residues Gly^{36} – Asp^{53}), which is folded toward the core of the protein, is shown in orange. The atomic root-mean square deviation (rmsd) about the mean of coordinates for nine α helices was 0.6 ± 0.1 Å for backbone and 1.2 ± 0.1 Å for all heavy atoms. No distance and dihedral restraints are consistently violated more than 0.4 Å and 5°, respectively. In addition, the quality factors for the structure as defined by the dipolar restraints ($Q_{dipolar}$) (Ottiger and Bax, 1999) were 0.5 ± 0.1.

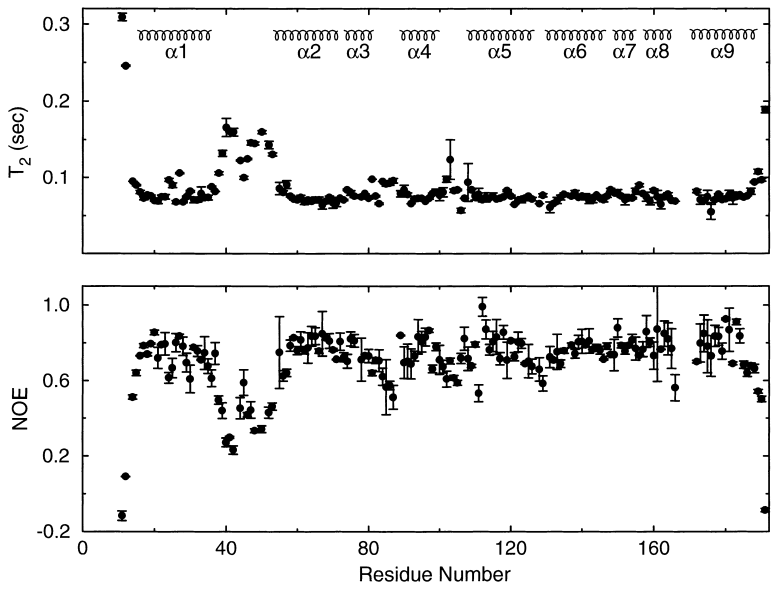

Figure 2. Backbone Dynamics of Bax

Transverse relaxation (T_2) (Barbato et al., 1992) and steady state heteronuclear $^{15}N\{^1H\}$-NOE (Grzesiek and Bax, 1993) for the backbone amides of Bax are plotted as a function of residue number. Higher ^{15}N T_2 and lower $^{15}N\{^1H\}$-NOE indicate high mobility regions, which include N-terminal 12 residues, and the loop between α1 and α2 except residues Glu^{44}–Ala^{46}, the loop between α3 and α4, and C-terminal four residues.

values which are negative, but higher than the average values for residues in the rest of this loop (Muchmore et al., 1996), suggesting that it is also less mobile. A similar variation in the backbone dynamic of N-terminal long loop in the HIV-1 protein Nef was also observed, with residues in the vicinity of the HIV-1 protease cleavage site having restricted motion preceded and followed by high internal mobility regions (Grzesiek et al., 1997). This central restriction in mobility contrasts with the long loop found in Bid that shows equal mobility for the entire loop (McDonnell et al., 1999). This loop in Bid includes the cleavage site for caspases thought to activate this proapoptotic protein (Li et al., 1998; Luo et al., 1998; Chou et al., 1999; McDonnell et al., 1999). The short loop between α8 and α9 of Bax is solvent-exposed, and the amide protons of two residues (Thr^{167}, Thr^{169}) exchange rapidly with solvent and are not observable. The lengths of these three flexible regions, the N-terminal tail (15 residues for Bax, 3 residues for Bcl-x_L), the long loop between α1 and α2 (18 residues for Bax, 63 for Bcl-x_L), and the loop between α8 and α9 (5 residues for Bax, 18 for Bcl-x_L), are quite different in Bax and Bcl-x_L.

The rest of the structure of Bax is almost identical to that of Bcl-x_L (Figure 3). Pairwise backbone root mean square (rms) shift between Bax and Bcl-x_L was calculated using the corresponding eight helices, excluding α9 which was deleted in the Bcl-x_L structure. The pairwise rms difference between Bax and Bcl-x_L is 3.2 Å. A smaller rms shift value of 2.3 Å was obtained for Bax and the Bcl-x_L–Bak peptide complex. Bid, a member of the third Bcl-2 subfamily, also consists of eight α helices (Chou et al., 1999; McDonnell et al., 1999). However, similarities between Bax and Bid (pairwise rms shift = 5.0 Å) or Bcl-x_L and Bid (pairwise rms shift = 4.2 Å) are much harder to discern, where pairwise rms shift values were calculated using further exclusion of α8 which does not exist in Bid. The high similarity in Bax and Bcl-x_L structures contrasts with the low (20%) percentage identity of their amino acid sequences, which is concentrated in three domains, BH1, BH2, and BH3 (Figure 3).

The BH4 domain in Bcl-x_L comprises helix α1. A similar helix is also present in Bax (Figure 3A) although a BH4 domain was not predicted by the amino acid sequence. The relative orientation of this helix with respect to the rest of the protein in Bax and Bcl-x_L is identical, albeit the length of helix α1 in Bax is longer by three residues. Earlier studies have shown that a portion of helix α1, residues Pro^{13}–Ile^{19}, is hidden in cytosolic form of Bax and becomes accessible to antibody binding after membrane insertion during apoptosis (Nechushtan et al., 1999). This indicates that a structural change that exposes helix α1 occurs during apoptosis.

Small differences between Bax and Bcl-x_L are observed in the relative orientations of helices α2, α3, and α4, which surround a hydrophobic pocket in Bcl-x_L. Helix α2 encompasses the BH3 domain that seems to be a functionally important region for interaction between members of the Bcl-2 family. This helix in the Bcl-x_L and the Bcl-x_L–Bak peptide structures is packed closer to the hydrophobic core of the protein than it is in Bax. In addition, this helix in the Bcl-x_L–peptide complex is elongated compared to the free Bcl-x_L or Bax structures

(B) A ribbon representation of an averaged minimized NMR structure for Bax. Helices are distinguished by different colors. Residues S16-A35, A54-D71, M74-A81, R89-M99, G108-C126, P130-E146, L149-D154, W158-Y164, W170-W188 make up helices α1, α2, α3, α4, α5, α6, α7, α8, α9, respectively.

(C) Amino acid sequence alignment between Bax and Bcl-x_L based on their structures. The BH1, BH2, BH3, and BH4 domains are indicated by cyan, magenta, red, and purple, respectively. Formation of a C-terminal helix with the same length (19 residues) as the Bax C-terminal helix is predicted for Bcl-x_L by amino acid sequence alignment. Italic characters indicate the residues deleted in the structural studies for Bcl-x_L.

(D) Multiple sequence alignment of conserved BH3 domain among Bcl-2 family proteins. Highly conserved residues are marked by asterisks.

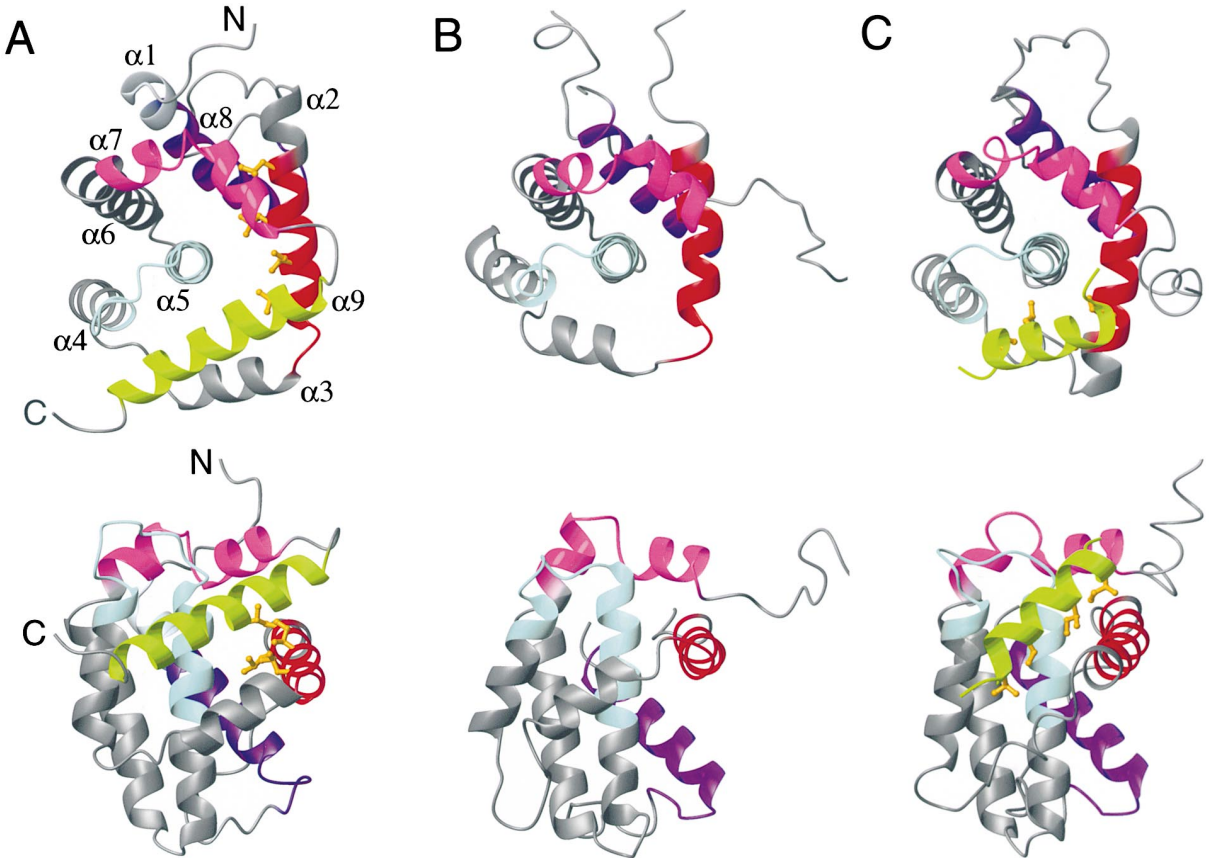

Figure 3. Structure Comparison between Bax and Bcl-x_L

Two different views of (A) Bax, (B) Bcl-x_L, and (C) Bcl-x_L complexed with Bak BH3 peptide are presented, a view straight down the central hydrophobic helix α5 (top panels) and a view from the side of the protein (bottom panels). The atomic coordinates of Bcl-x_L and the Bcl-x_L–peptide complex were obtained from the Protein Data Bank with ID codes 1MAZ and 1BXL, respectively. The BH1, BH2, BH3, and BH4 domains are shown in cyan, magenta, red, and blue, respectively. Helix α1 in Bax, which corresponds to BH4 containing helix in Bcl-x_L, is shown in purple. The C-terminal helix of Bax and the Bak BH3 peptide are shown in green. The C-terminal 24 residues of Bcl-x_L were deleted in both structural studies of free and complexed Bcl-x_L. The side chain of hydrophobic residues of Bak BH3 peptide (Val^{74}, Leu^{78}, Ile^{81}, and Ile^{85}) for stabilizing the complex formation between Bcl-x_L and Bak BH3 peptide and those of corresponding hydrophobic residues of Bax BH3 domain (Leu^{60}, Leu^{63}, Ile^{66}, Leu^{70}) are represented by balls and sticks.

by six residues. Helix α3 in free Bcl-x_L is shifted toward the hydrophobic pocket compared to that of Bax, and in the Bcl-x_L–Bak peptide complex, this helix is shortened by three residues compared to those of Bax and free Bcl-x_L. The orientation of helix α4 in Bcl-x_L is also slightly different than in Bax. The interhelical angle between helix α4 and the central hydrophobic helix α5 is 11° in Bax, 39° in Bcl-x_L, and 24° in the Bcl-x_L–Bak peptide complex. The BH1 domain bridges the helices α4 and α5 (Figure 3). The orientation and lengths of the rest of the helices, α5, α6, α7, and α8 of Bax, free Bcl-x_L, and complexed Bcl-x_L are very similar. The helices α7 and α8 make up the conserved BH2 domain (Figure 3).

The C-terminal hydrophobic region of Bax is the putative transmembrane domain. A portion of this C-terminal region forms helix α9. The helix α9 of Bax is located in the hydrophobic pocket in a manner similar to the way the Bak BH3 peptide binds to the Bcl-x_L, although the directional sense of the peptide is opposite to that of the C-terminal helix of Bax (Figures 3A and 3C). The C-terminal 24 residues in Bcl-x_L were deleted (Figures 3B and 3C), and the absence of this part of the protein results in the exposure of the hydrophobic pocket. The shift of helices α2, α3, α4 in Bcl-x_L can be in part accounted for by their effort in reducing the exposed hydrophobic surface area. The short Bak peptide or its absence does not hinder helix α2, α3, and α4 from packing closely to the core. In Bax, the long C-terminal helix defines the orientation and packing of these helices. This hydrophobic pocket of Bcl-x_L binds peptides from the BH3 domain of Bak (Figure 3C), and had been proposed to provide the site for possible dimerization between antiapoptotic Bcl-x_L and the BH3 domain of proapoptotic counterparts (Sattler et al., 1997).

Structural Change Associated with Increase in pH

It has been reported that a rapid increase in intracellular pH associated with cytokine withdrawal triggers Bax translocation into mitochondria (Khaled et al., 1999). This leads to the hypothesis that Bax undergoes a conformational change at pH 7.8 or higher. In order to test this hypothesis, we acquired a series of 2D (^1H-^{15}N)

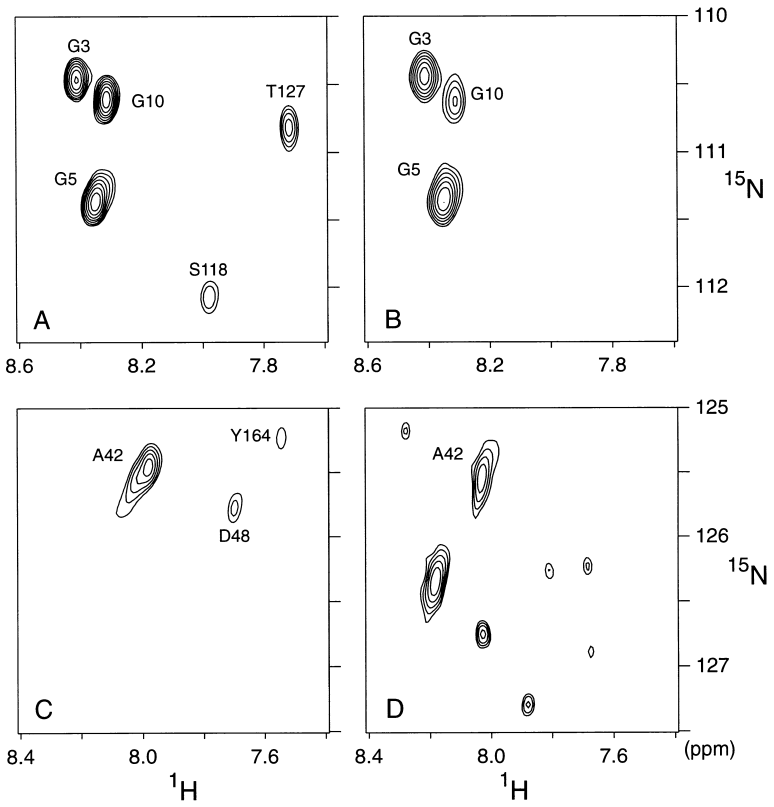

Figure 4. Spectral Changes of Bax upon Addition of β-octylglucoside

Trosy spectra of the downfield ^{15}N region of Bax (A) in the absence and (B) in the presence of β-octylglucoside. The upfield ^{15}N regions of the same spectra of Bax before and after the addition of β-octylglucoside are shown in (C) and (D), respectively.

HSQC spectra of Bax at various pH values from 6 to 8. No significant shift in resonance peaks was detected within this range of pH values (data not shown). This indicates the absence of conformational change of Bax at high pH.

Another proposed mechanism for Bax function in promoting apoptosis is through self-aggregation (Oltvai et al., 1993). It is perhaps possible that an increase or decrease in intracellular pH could change the monomeric form of Bax found under the NMR sample condition to a higher state of aggregation. In order to check for this possibility, we have measured nonspecific backbone ^{15}N T_2 (data not shown), which directly reflects the effective size of the system, at various pH values between pH 6 and 8. The ^{15}N T_2 values measured did not vary significantly with an average value of 76 $\pm$ 5 ms. This suggests that Bax stays as a monomer at a wide range of potential intracellular pH values.

Effect of Detergents on the Structure of Bax

Several detergents appear to induce complex formation of Bax. It has been shown that Bax forms homodimers as well as heterodimers with Bcl-x_L in the presence of various detergents, such as Triton X-100, Tween 20, and β-octylglucoside (Hsu and Youle, 1997). In addition, the formation of Bax oligomers has been reported in the presence of β-octylglucoside (Antonsson et al., 2000). In order to try to elucidate detailed structural changes in Bax, we have monitored changes in its 2D (^1H-^{15}N) TROSY (Pervushin et al., 1997) spectrum at various β-octylglucoside concentrations. Dramatic changes can clearly be observed in TROSY spectra of Bax (Figure 4). No significant changes were observed in Bax spectra at a β-octylglucoside concentration of 0.2%. However, an abrupt change in the spectrum was observed at 0.6%. As expected, considerable broadening of the resonance peaks was observed associated with a significant increase in the effective molecular size. The broadening is severe enough to prohibit the observation of all resonance peaks in the spectrum. Resonances belonging to residues in the N-terminal flexible region (at least up to residue Gly[11]) and the loop between helices α1 and α2 stay relatively sharp and intense. This indicates that these regions are still flexible and most likely solvent exposed even in the larger molecular weight complex. Within the small percentage of resonances that can be observed, significant changes can clearly be seen in comparison to the detergent free spectrum. This suggests that Bax undergoes significant conformational change in the presence of the detergent. At this time, no identification of these resonances can be made due to the very abrupt change in the spectrum of Bax with the addition of detergent as well as the severe line broadening because of the large effective size of the molecule.

Apoptosis Initiation by Bax through Its C Terminus

The structure of Bax implies that the disruption of the α9 helix conformation out of the hydrophobic pocket will play an important role in apoptosis initiation. To examine the possible consequences of destabilizing these interactions, several chimeras between Bax and Bcl-x_L were constructed (Figure 5). The green fluorescence protein (GFP) was used as a tag for all these constructs to report their subcellular localization. The

A

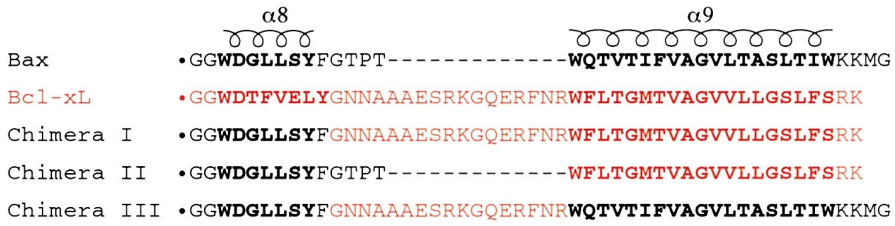

B

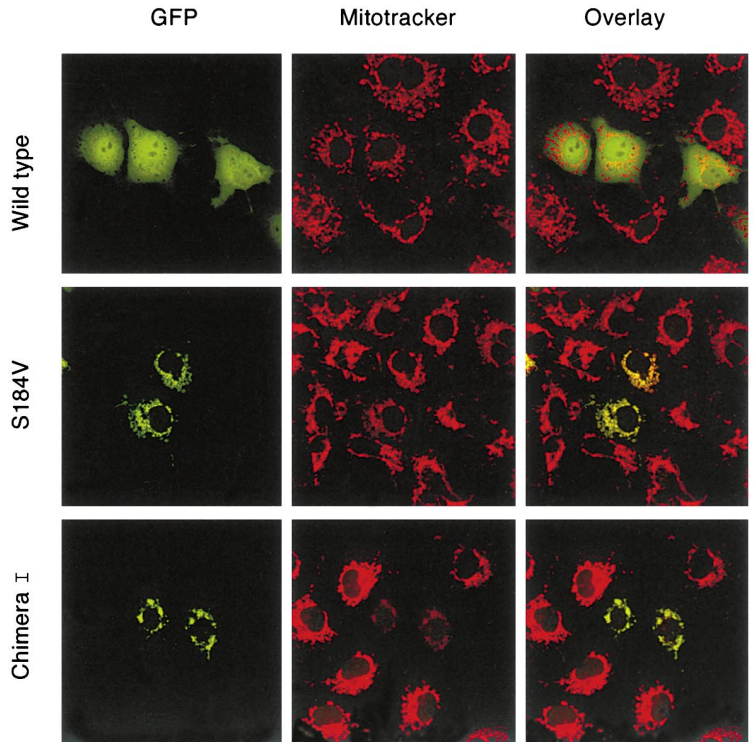

Figure 5. Subcellular Localization of Bax Constructs

(A) Design of Bax–Bcl-x_L chimeric proteins. Red color indicates that the composition originates in Bcl-x_L.
(B) Confocal microscopy of living cells expressing different Bax constructs.

S184V mutant of Bax and wild-type Bax were used as positive and negative controls of mitochondrial association, respectively. As previously reported, the S184V mutant of Bax constitutively associates to the mitochondria (Nechushtan et al., 1999). This is shown by the overlap of the green GFP and red mitotracker confocal images (Figure 5). This confirms the cellular localization of S184V Bax mutant in the mitochondria.

Chimera I consists of N-terminal 166 residues of Bax and C-terminal 37 residues of Bcl-x_L, containing the predicted C-terminal helix. The conformation of the C-terminal helix of Bcl-x_L defines the protein cellular localization such that a large percentage of it is found in the mitochondria (Hsu et al., 1997; Wolter et al., 1997). It was expected that Bax containing the Bcl-x_L C-terminal helix would adopt a similar distribution. Indeed, chimera I exhibited constitutive mitochondria localization (Figure 5). The mitochondria-localized Bax appeared to induce a loss of membrane potential as the signal intensity of mitotracker of the transfected cells was lower than that of nontransfected cells. In addition to different C-terminal helices, the difference in the length of the loops preceding the C-terminal helix in Bax and Bcl-x_L could contribute to the stability of the C-terminal helix packing and thus cellular localization. Therefore, chimera II, where only the C-terminal helix of Bax was replaced, and chimera III, where only the loop was replaced, were also tested. Chimera II exhibited similar results as chimera I (data not shown). However the confocal images of chimera III were indistinguishable from those of the wild-type Bax (data not shown). These results suggest that the length of the loop preceding helix α9 plays no important role in defining the different α9 helix conformations of Bax and Bcl-x_L. Furthermore, the cellular localization of these chimeras correlates with Bax toxicity. All constructs that contain the Bcl-x_L C-terminal helix

and more readily associate with mitochondria showed a significant increase in cellular toxicity.

Discussion

Regulation of Dimer Formation

The BH3 domain appears to be essential for the activity of proapoptotic members in the Bcl-2 family. The BH3 domain also has been shown to be required for dimer formation among Bcl-2 proteins. The BH3 domain of Bax is in helix α2. The side chains of the hydrophobic residues in the BH3 domain of Bax (Leu^{59}, Leu^{63}, Ile^{66}, and Leu^{70}) (Figure 3A) proposed to be important for dimer formation are oriented toward the center hydrophobic core of the protein. Therefore, the previously proposed dimerization model (Sattler et al., 1997) requires a conformational change of Bax in which the helix α2 rotates about its axis to expose these residues away from the hydrophobic core of the protein. Although this helix was predicted to be flanked by highly flexible loops (Sattler et al., 1997), in Bax, the loop between helices α2 and α3 is rigid, as the $^{15}N\{^1H\}$-NOE values are the same as those of residues in the helical regions of the protein (Figure 2). In addition, the rotation of this helix will also disrupt the hydrophobic core formed by helices α1, α4, α5, and α6. Considering that the side opposite to the proposed interaction site of helix α2 contains mostly polar residues, this rotation will lead to a very energetically unfavorable conformation. Therefore, rotation of this helix would require considerable rearrangements of other parts of the protein.

Bax has been suggested to undergo a conformational change under high pH condition (Khaled et al., 1999). Other studies show a decrease in pH during apoptosis (Li and Eastman, 1995; Matsuyama et al., 2000). Our study shows that no significant changes in the spectra or backbone ^{15}N T_2 values were observed for pH values between 6 and 8. Thus, no conformational rearrangement or change in the aggregation state of Bax in solution was present within potential intracellular pH range. This suggests that there is no direct link between intracellular pH change and Bax translocation into the mitochondria.

The ability of detergents to induce complex formation of Bax is well established (Hsu and Youle, 1997; Antonsson et al., 2000). Our detergent titration study confirms these observations. One of the biggest questions was whether this transformation would be associated with considerable conformational change of Bax. Our data show that the presence of detergent triggers Bax to form higher aggregates. It was not possible to estimate the effective size of the aggregates, since NMR cannot easily distinguish between the size of the detergent-formed micelle and the protein aggregates. However, it has been suggested that Bax would form an oligomer composed of six to eight Bax molecules in the presence of detergent (Antonsson et al., 2000), and our data certainly do not dispute this observation. In addition, our results also revealed at least two novel findings. First, our data provide direct evidence that there is a substantial conformational change upon oligomerization of Bax. Second, the N-terminal region, proposed to be important for oligomer formation and apoptosis initiation, remains flexible and solvent exposed in the presence of detergent. The long loop between helices α1 and α2 also shows the same behavior. All of these taken together would suggest that the primary driving force for aggregation would be changes in the helical packing, and the conformations of these loops seem to play no major role.

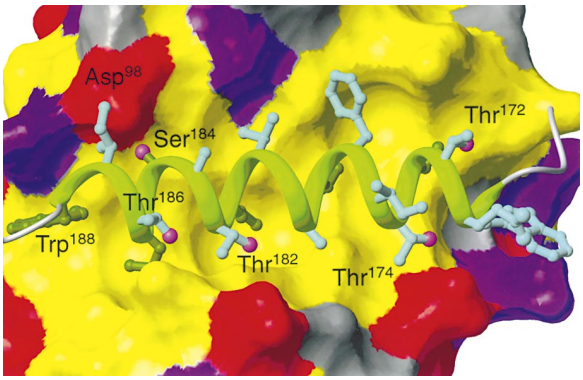

Figure 6. The Orientation of the C-terminal Helix

A close-up view of the Bax C-terminal helix and the hydrophobic pocket is shown. The side chains of the residues in the C-terminal helix are represented by balls and sticks. Solvent exposed side chains are shown in cyan. Magenta balls represent oxygen atom in threonines and serine. A surface representation of the pocket is colored red, purple, and yellow to represent negative, positive, and hydrophobic residues, respectively.

The structural similarity between Bax and Bcl-x_L suggests that functional models put forward for one might be applicable for the other. In other words, the hydrophobic pocket of Bax should be capable of accepting a BH3 domain of other Bcl-2 family members. Indeed, it has been shown that Bid cooperates with Bax to cause mitochondrial dysfunction, and Bid binding to Bax requires the Bid BH3 domain (Wang et al., 1996; Desagher et al., 1999). However, the C-terminal helix α9 of Bax occupies the hydrophobic pocket. The interactions between the C-terminal helix and the pocket are mainly hydrophobic (Figure 6), and no electrostatic interactions were observed that might stabilize the packing of this helix. The hydroxyl group in the side chain of Ser^{184} points toward the core of the protein and appears to form a hydrogen bond to the carboxyl group of Asp^{98} in helix α4. These contacts between the Bax C terminus and the BH3 binding pocket would prevent dimer formation at this site. It is very unlikely that a BH3 domain of another Bcl-2 family member alone could compete with the C-terminal helix of Bax for binding to its BH3 pocket. Therefore, dimerization via this pocket cannot occur in the cytosol without the presence of an energy-driven triggering process to disengage helix α9.

Intracellular Localization

The C-terminal helix, composed mostly of hydrophobic residues, is also rich in amino acids containing hydroxyl groups (Thr^{172}, Thr^{174}, Thr^{182}, Ser^{184}, and Thr^{186}). With one exception (Ser^{184}), these polar residues are solvent exposed (Figure 6). The conformation of the C-terminal helix α9 contributes to the solubility of Bax by effectively reducing the exposed hydrophobic surface, consistent

with the subcellular localization of monomeric Bax in the cytosol of healthy cells (Hsu and Youle, 1998), even though Bax is homologous to other membrane-integrated Bcl-2 proteins.

Upon induction of apoptosis (Hsu et al., 1997; Wolter et al., 1997) or upon perturbation of its structure (Goping et al., 1998; Gross et al., 1998; Nechushtan et al., 1999), Bax binds mitochondria, apparently via its C-terminal helix, as deletion of the last five or more amino acids prevents mitochondrial binding (Wolter et al., 1997; Nechushtan et al., 1999). Extensive mutagenesis studies have suggested that the sequence of the C terminus is critical for mitochondrial docking of Bax. When Ser^{184} is either deleted or replaced by a Val or Ala, Bax constitutively associates with mitochondrial membranes (Nechushtan et al., 1999). Elimination of the Ser^{184}–Asp^{98} hydrogen bond promotes dissociation of the C-terminal helix from the hydrophobic pocket, making it more accessible to the mitochondrial membrane. This result was confirmed with the confocal images of GFP tagged Bax S184V mutant. On the other hand, replacement of Ser^{184} with Lys, Glu, or Asp (Nechushtan et al., 1999) or Trp^{188} with Ala or Leu (A. Nechushtan, C.L. Smith, and R.J. Youle, unpublished data) abolished Bax translocation from the cytosol to the mitochondria. These two residues (Ser^{184} and Trp^{188}), side chains of which are oriented into the pocket, seem to be close to the actual mitochondrial binding site of Bax. Therefore, the conformational change that allows the C terminus to enter mitochondrial membranes must disengage helix α9 from the protein core, and thus expose the hydrophobic BH3 binding pocket to participate in dimer formation.

The absence of the last 24 residues in both of the Bcl-x_L and Bcl-x_L-peptide complex structures prohibits detailed comparison of the C-terminal of Bax and Bcl-x_L. However, based on the similarity of the core structures between Bax and Bcl-x_L as well as their amino acid sequence homology, the C-terminal helix of Bcl-x_L, at least the cytosolic form, can be expected to adopt the same conformation as that of Bax.

The results of the chimera experiments prove that residue composition of the C-terminal helix plays an important role in cellular localization of Bax. Bax containing the C-terminal helix of Bcl-x_L is constitutively associated with the mitochondria and has higher toxicity. The effects could be attributed to the mismatch between the Bcl-x_L C-terminal helix and Bax hydrophobic pocket, thus destabilizing their interaction. Alternatively, the Bcl-x_L C-terminal helix could have higher mitochondria affinity and bind mitochondria without apoptosis signal. Nevertheless, the C-terminal helix clearly holds the determinant for cellular localization of these proteins. If the C-terminal helix had any direct consequence to toxicity, one would expect Bax constructs containing the antiapoptotic Bcl-x_L C-terminal helix would be less toxic than wild-type Bax. The results are exactly the opposite suggesting that the C-terminal does not directly contribute to the protein toxicity. It merely facilitates mitochondria access that is the first determinant step in apoptosis.

The result of this study only addresses factors that are important for mitochondria binding or docking of Bax. Currently our data cannot provide detailed information on the conformation of Bax after insertion into the mitochondria. This aspect of Bax function in apoptosis certainly provides challenges for future studies.

The opposing biological functions of Bax and Bcl-x_L are in absolute contrast to their surprisingly similar structures. Some differences within the flexible regions may distinguish their activities. It is interesting that the loop prior to helix α9 is much shorter in Bax than in either Bcl-2 or Bcl-x_L; however, our experiments indicate that it does not help to retain helix α9 in the pocket and maintain Bax in the cytosol. The absence of further distinction between their structures would suggest that other components in the apoptosis pathways or an altered structure after insertion into mitochondrial membranes might be important in differentiating the functional roles of these two proteins. It is now apparent that a conformational change involving the C-terminal helix is prerequisite to initiate Bax mitochondrial docking. The structural changes in Bax associated with apoptosis that displace the C-terminal helix from the BH3 binding pocket, allowing this helix to interact with the mitochondrial membrane, could also promote dimer formation. Therefore, the C-terminal helix of Bax provides an autoinhibitory mechanism to prevent exposure of the BH3 binding pocket and to inhibit mitochondrial docking prior to apoptosis.

A number of different membrane proteins outside the Bcl-2 family, such as the vesicle fusion protein (VAMP-1), the protein tyrosine phosphatase (PTP-1), and cytochrome b5, are synthesized in the cytosol and insert posttranslationally into membranes via C-terminal hydrophobic domains. How these proteins recognize the appropriate organelle, dock to membranes, and insert into lipid bilayers to become integral membrane proteins is unknown. Interestingly, a number of these proteins exist in both cytosolic and membrane-inserted conformations (Kim et al., 1997; Calera et al., 2000). It is conceivable that the conformational rearrangement described above for Bax is a general mechanism controlling the partitioning of this class of proteins.

Experimental Procedures

NMR Sample

cDNA of human Bax was subcloned into NdeI/SapI site of pTYB1 vector (New England Biolabs Inc., Beverly, MA). The resulting plasmid pTYB1-Bax encodes a fusion protein of Bax and chitin binding protein, which can be cleaved off to obtain Bax with neither any extra amino acid nor truncation. *Escherichia coli* BL21(DE3) harboring pTYB1-Bax was cultured in minimal medium containing $^{15}NH_4Cl$ without or with [U-^{13}C] glucose to produce uniformly ^{15}N- or ^{15}N-, ^{13}C- labeled protein. Recombinant proteins were isolated from the cytosol by a chitin affinity chromatography according to the protocol provided from the manufacturer (New England Biolabs Inc.), and further purified by an ion-exchange chromatography on a mono-Q column (Amersham Pharmacia Biotech, Piscataway, NJ). The typical yield of 0.25 mg/l culture can reproducibly be obtained. No detergents were used in any step of the protein purification. The last ion-exchange column was essential in eliminating trace amounts of impurity that are detrimental to the solubility of the protein. All NMR samples contained 0.5–1.0 mM protein in 10 mM Tris-acetate, pH 6.0 and 2 mM dithiothreitol in 90% H_2O/10% D_2O or 100% D_2O.

NMR Spectroscopy

All NMR spectra were acquired at 32°C on Bruker 600 or 800 MHz NMR spectrometers. The following experiments were used for assignments of ^{1}H, ^{13}C, and ^{15}N resonances: CBCA(CO)NH, HNCACB, HBHA(CO)NH, HNCO, and 3D HCCH-TOCSY. Proton homonuclear

NOEs were obtained from 3D ^{15}N-separated NOESY, 4D ^{15}N/^{13}C-separated NOESY, and 4D ^{13}C/^{13}C-separated NOESY experiments. Residual dipolar couplings for backbone NH, $C^{\alpha}H^{\alpha}$, and $C^{\alpha}C'$ vectors and CH vectors were calculated from the difference in corresponding scalar (J) couplings measured in the presence and absence of Pf1 phage (12 mg/ml) (Hansen et al., 1998). Modified versions of CT-HNCO experiments were used to measure the NH and $C^{\alpha}C'$ scalar couplings. The $C^{\alpha}H^{\alpha}$ couplings were measured using BRCT-3DJ as well as CT-[H]CA[CO]NH experiments.

Structure Calculation

Regions of regular secondary structure were determined based on secondary C^{α} chemical shifts and medium range NOE patterns. The TALOS program (Cornilescu et al., 1999) was used to predict dihedral angles ϕ and ψ. The statistically significant angles in regular secondary structure were used as structural restraints with at least 30° margins. Generic hydrogen bond distance restraints were employed for α-helical regions. Peak intensities from NOESY experiments were translated into a continuous distribution of proton–proton distances. Structures of Bax were calculated by a distance geometry and simulated annealing protocol (Kuszewski et al., 1992) using the program X-PLOR (Brünger, 1992) modified to incorporate dipolar coupling restraints (Tjandra and Bax, 1997). Structure calculations employed 1616 interresidue and 860 intraresidue proton–proton distance restraints, 178 hydrogen bond distance restraints, 123 ϕ and 123 ψ angle restraints, 156 NH, 164 $C^{\alpha}H^{\alpha}$, 147 $C^{\alpha}C'$, and 100 side chain CH dipolar couplings. All molecule illustrations were produced using the program MOLMOL (Koradi et al., 1996).

Detection of Bax Constructs in Living Cells

pEGFP-C3-Bax and pEGFP-C3-Bax (S184V) constructs have been described previously (Wolter et al., 1997; Nechushtan et al., 1999). The chimeric proteins between Bax and Bcl-x_L were synthesized by PCR using cDNA for human Bax and human Bcl-x_L as templates. The DNA fragments encoding the chimeras were generated by an overlap extension PCR protocol with appropriate primers. Primer 1 (ctc tcc tac ttt ggg aac aat gca gca) and primer 2 (tgc tgc att gtt ccc aaa gta gga gag) were used to prepare chimera I, primer 3 (ggg acg ccc acg tgg ttc ctg acg ggc) and primer 4 (gcc cgt cag gaa cca cgt ggg cgt ccc) were for chimera II, and all four primers were for chimera III. The amplified fragments were cloned into pEGFP-C3 vector (Clontech Laboratories, Inc., Palo Alto, CA).

Cos-7 green monkey renal epithelia cells (American Type Culture Collection, Rockville, MD) were grown in Dulbecco's modified Eagle's medium supplemented with 10% heat-inactivated fetal calf serum at 37°C in 5% CO_2. Cells were transfected with pEGFP-Bax constructs using FuGENE transfection reagent (Roche Diagnostics GmbH, Mannheim, Germany) as described by the manufacturer using 1 μg of plasmid DNA per dish. After 18–24 hr, confocal microscopy of live cells was performed by incubation with 20 ng/ml of a mitochondrion-specific dye (Mitotracker red CMXRos; Molecular Probes Inc., Eugene, OR). Images were collected on a model IX70 microscope (Olympus America Inc., Melville, NY). The 488 and 568 nm lines of krypton/argon laser were used for fluorescence excitation of GFP and mitotracker red CMXRos, respectively. For toxic constructs, observation was carried out at 6–10 hr after transfection.

Acknowledgments

We thank Yi-Te Hsu, Ad Bax, Martha Vaughan, and John Collier for discussions and comments.

Received June 13, 2000; revised September 27, 2000.

References

Adams, J.M., and Cory, S. (1998). The Bcl-2 protein family: arbiters of cell survival. Science *281*, 1322–1326.

Antonsson, B., Montessuit, S., Lauper, S., Eskes, R., and Martinou, J.C. (2000). Bax oligomerization is required for channel-forming activity in liposomes and to trigger cytochrome c release from mitochondria. Biochem. J. *345*, 271–278.

Barbato, G., Ikura, M., Kay, L.E., Pastor, R.W., and Bax, A. (1992). Backbone dynamics of calmodulin studied by ^{15}N relaxation using inverse detected two-dimensional NMR spectroscopy: the central helix is flexible. Biochemistry *31*, 5269–5278.

Brünger, A.T. (1992). X-PLOR Version 3.1 (New Haven, CT: Yale University).

Calera, M.R., Vallega, G., and Pilch, P.F. (2000). Dynamics of protein-tyrosine phosphatases in rat adipocytes. J. Biol. Chem. *275*, 6308–6312.

Chou, J.J., Li, H., Salvesen, G.S., Yuan, J., and Wagner, G. (1999). Solution structure of BID, an intracellular amplifier of apoptotic signaling. Cell *96*, 615–624.

Clore, G.M., Gronenborn, A.M., and Bax, A. (1998). A robust method for determining the magnitude of the fully asymmetric alignment tensor of oriented macromolecules in the absence of structural information. J Magn. Reson. *133*, 216–221.

Cornilescu, G., Marquardt, J.L., Ottiger, M., and Bax, A. (1998). Validation of protein structure from anisotropic carbonyl chemical shifts in a dilute liquid crystalline phase. J. Am. Chem. Soc. *120*, 6836–6837.

Cornilescu, G., Delaglio, F., and Bax, A. (1999). Protein backbone angle restraints from searching a database for chemical shift and sequence homology. J. Biomol. NMR *13*, 289–302.

Desagher, S., Osen-Sand, A., Nichols, A., Eskes, R., Montessuit, S., Lauper, S., Maundrell, K., Antonsson, B., and Martinou, J.C. (1999). Bid-induced conformational change of Bax is responsible for mitochondrial cytochrome c release during apoptosis. J. Cell Biol. *144*, 891–901.

Goping, I.S., Gross, A., Lavoie, J.N., Nguyen, M., Jemmerson, R., Roth, K., Korsmeyer, S.J., and Shore, G.C. (1998). Regulated targeting of BAX to mitochondria. J. Cell Biol. *143*, 207–215.

Green, D.R., and Reed, J.C. (1998). Mitochondria and apoptosis. Science *281*, 1309–1312.

Gross, A., Jockel, J., Wei, M.C., and Korsmeyer, S.J. (1998). Enforced dimerization of BAX results in its translocation, mitochondrial dysfunction and apoptosis. EMBO J. *17*, 3878–3885.

Gross, A., McDonnell, J.M., and Korsmeyer, S.J. (1999). BCL-2 family members and the mitochondria in apoptosis. Genes Dev. *13*, 1899–1911.

Grzesiek, S., and Bax, A. (1993). Amino-acid type determination in the sequential assignment prodedure of uniformly ^{13}C/^{15}N-enriched proteins. J. Biomol. NMR *3*, 185–204.

Grzesiek, S., Bax, A., Hu, J.S., Kaufman, J., Palmer, I., Stahl, S.J., Tjandra, N., and Wingfield, P.T. (1997). Refined solution structure and backbone dynamics of HIV-1 Nef. Protein Sci. *6*, 1248–1263.

Hansen, M.R., Mueller, L., and Pardi, A. (1998). Tunable alignment of macromolecules by filamentous phage yields dipolar coupling interactions. Nat. Struct. Biol. *5*, 1065–1074.

Hsu, Y.T., and Youle, R.J. (1997). Nonionic detergents induce dimerization among members of the Bcl-2 family. J. Biol. Chem. *272*, 13829–13834.

Hsu, Y.T., and Youle, R.J. (1998). Bax in murine thymus is a soluble monomeric protein that displays differential detergent-induced conformations. J. Biol. Chem. *273*, 10777–10783.

Hsu, Y.T., Wolter, K.G., and Youle, R.J. (1997). Cytosol-to-membrane redistribution of Bax and Bcl-X_L during apoptosis. Proc. Natl. Acad. Sci. USA *94*, 3668–3672.

Khaled, A.R., Kim, K., Hofmeister, R., Muegge, K., and Durum, S.K. (1999). Withdrawal of IL-7 induces Bax translocation from cytosol to mitochondria through a rise in intracellular pH. Proc. Natl. Acad. Sci. USA *96*, 14476–14481.

Kim, P.K., Janiak-Spens, F., Trimble, W.S., Leber, B., and Andrews, D.W. (1997). Evidence for multiple mechanisms for membrane binding and integration via carboxyl-terminal insertion sequences. Biochemistry *36*, 8873–8882.

Koradi, R., Milleter, M., and Wüthrich, K. (1996). MOLMOL: a program for display and analysis of macromolecular structures. J. Mol. Graph. *14*, 51–55.

Kuszewski, J., Nilges, M., and Brünger, A.T. (1992). Sampling and

efficiency of metric matrix distance geometry: a novel partial metrization algorithm. J. Biomol. NMR *2*, 33–56.

Li, J., and Eastman, A. (1995). Apoptosis in an interleukin-2-dependent cytotoxic T lymphocyte cell line is associated with intracellular acidification. Role of the Na^+/H^+-antiport. J. Biol. Chem. *270*, 3203–3211.

Li, H., Zhu, H., Xu, C.J., and Yuan, J. (1998). Cleavage of BID by caspase 8 mediates the mitochondrial damage in the Fas pathway of apoptosis. Cell *94*, 491–501.

Luo, X., Budihardjo, I., Zou, H., Slaughter, C., and Wang, X. (1998). Bid, a Bcl2 interacting protein, mediates cytochrome c release from mitochondria in response to activation of cell surface death receptors. Cell *94*, 481–490.

Matsuyama, S., Llopis, J., Deveraux, Q.L., Tsien, R.Y., and Reed, J.C. (2000). Changes in intramitochondrial and cytosolic pH: early events that modulate caspase activation during apoptosis. Nat. Cell. Biol. *2*, 318–325.

McDonnell, J.M., Fushman, D., Milliman, C.L., Korsmeyer, S.J., and Cowburn, D. (1999). Solution structure of the proapoptotic molecule BID: a structural basis for apoptotic agonists and antagonists. Cell *96*, 625–634.

Minn, A.J., Kettlun, C.S., Liang, H., Kelekar, A., Vander Heiden, M.G., Chang, B.S., Fesik, S.W., Fill, M., and Thompson, C.B. (1999). Bcl-xL regulates apoptosis by heterodimerization-dependent and -independent mechanisms. EMBO J. *18*, 632–643.

Muchmore, S.W., Sattler, M., Liang, H., Meadows, R.P., Harlan, J.E., Yoon, H.S., Nettesheim, D., Chang, B.S., Thompson, C.B., Wong, S.L., et al. (1996). X-ray and NMR structure of human Bcl-x_L, an inhibitor of programmed cell death. Nature *381*, 335–341.

Nechushtan, A., Smith, C.L., Hsu, Y.T., and Youle, R.J. (1999). Conformation of the Bax C-terminus regulates subcellular location and cell death. EMBO J. *18*, 2330–2341.

Oltvai, Z.N., Milliman, C.L., and Korsmeyer, S.J. (1993). Bcl-2 heterodimerizes in vivo with a conserved homolog, Bax, that accelerates programmed cell death. Cell *74*, 609–619.

Ottiger, M., and Bax, A. (1999). Bicelle-based liquid crystals for NMR-measurement of dipolar couplings at acidic and basic pH values. J. Biomol. NMR *13*, 187–191.

Ottiger, M., Delaglio, F., Marquardt, J.L., Tjandra, N., and Bax, A. (1998). Measurement of dipolar couplings for methylene and methyl sites in weakly oriented macromolecules and their use in structure determination. J. Magn. Reson. *134*, 365–369.

Pervushin, K., Riek, R., Wider, G., and Wüthrich, K. (1997). Attenuated T2 relaxation by mutual cancellation of dipole-dipole coupling and chemical shift anisotropy indicates an avenue to NMR structures of very large biological macromolecules in solution. Proc. Natl. Acad. Sci. USA *94*, 12366–12371.

Sattler, M., Liang, H., Nettesheim, D., Meadows, R.P., Harlan, J.E., Eberstadt, M., Yoon, H.S., Shuker, S.B., Chang, B.S., Minn, A.J., et al. (1997). Structure of Bcl-xL–Bak peptide complex: recognition between regulators of apoptosis. Science *275*, 983–986.

Tjandra, N., and Bax, A. (1997). Direct measurement of distances and angles in biomolecules by NMR in a dilute liquid crystalline medium. Science *278*, 1111–1114.

Wang, K., Yin, X.M., Chao, D.T., Milliman, C.L., and Korsmeyer, S.J. (1996). BID: a novel BH3 domain-only death agonist. Genes Dev. *10*, 2859–2869.

Wang, K., Gross, A., Waksman, G., and Korsmeyer, S.J. (1998). Mutagenesis of the BH3 domain of BAX identifies residues critical for dimerization and killing. Mol. Cell. Biol. *18*, 6083–6089.

Wolter, K.G., Hsu, Y.T., Smith, C.L., Nechushtan, A., Xi, X.G., and Youle, R.J. (1997). Movement of Bax from the cytosol to mitochondria during apoptosis. J. Cell Biol. *139*, 1281–1292.

Protein Data Bank Accession Number

The coordinates for the 20 lowest energy Bax structures have been deposited with the accession number 1F16.